Sandwich-like heat-resistance composite separators with tunable pore structure for high power high safety lithium ion batteries

Junli Shi, Tao Shen, Huasheng Hu, Yonggao Xia[*], Zhaoping Liu[*]

Ningbo Institute of Materials Technology Engineering (NIMTE), Chinese Academy of Sciences, Zhejiang 31520, PR China

HIGHLIGHTS

- Separators with a unique sandwich-like structure are developed.
- Excellent thermal stability and flame retardant ability contribute to higher battery safety.
- Separators exhibit superior cell performances than commercial PP separator.
- New insight into the influences of separators on the cell performances is proposed.

ARTICLE INFO

ABSTRACT

We demonstrate a new kind of composite separators. A unique feature of the separators is the three-tier structure, i.e. the crosslinked polyethylene glycol (PEG) skin layer being formed on both sides of the nonwoven separators by in-situ polymerization and the large pores in the interior of the nonwoven separators being remained. The surface pore structure and the thickness of the skin layer could be adjusted by controlling the concentration of the coating solution. The skin layer is proved to be able to provide internal short circuit protection, to contribute a more stable interfacial resistance and to alleviate liquid electrolyte leakage effectively, yielding an excellent cyclability. The remained large pores in the interior of the composite separators could provide an access for the fast transportation of lithium ions, giving rise to a very high ion conductivity. The polyimide (PI) nonwoven is employed to ensure enhanced thermal stability of the composite separators. More notably, the composite separators fabricated from the coating solution with a composition ratio of 20 wt% provide superior cell performances owing to the well-tailored microporous structure, comparing with the commercialized polypropylene (PP) separator, which show great promise for the application in the high power lithium ion batteries.

© 2014 Elsevier B.V. All rights reserved.

1. Introduction

The expanding applications, including (hydrid) electric vehicles and energy storage systems, have put forward higher requirements for lithium ion batteries [1,2]. High energy/power density, high-security have been an important developing trend [3]. Accordingly, the performances of the battery components, including cathode, anode and separator, are urgently needed to be improved. Thereinto, separator plays an important role in preventing the physical contact between the electrodes, retaining liquid electrolyte and conducting lithium ions. These features of the separator would largely influence battery safety and power density [4]. Currently, polyolefin based separators are widely used in commercialized lithium ion batteries due to their low price and chemical durability. However, their poor thermal stability and poor wettability have raised serious concerns on their capacity for the application in high power lithium ion batteries [5].

Various efforts have been done to overcome the drawbacks of polyolefin based separators, for example, introducing the inorganic or organic coating layer to enhance the thermal resistance and wettability [6,7]. Recently, heat-resistance nonwoven separators have also been developed [8,9]. The high porosity and excellent thermal properties have attracted considerable attention. This kind of separators is typically manufactured from heat-resistance engineering polymer, such as polyester (PET) [9], polyimide (PI) [10], polyacrylonitrile (PAN) [11] and so on, which usually own higher

* Corresponding authors. Tel./fax: +86 574 86685701.
  E-mail addresses: xiayg@nimte.ac.cn (Y. Xia), liuzp@nimte.ac.cn (Z. Liu).

melting temperature (>250 °C) than the traditional polyolefin based separators. When this kind of nonwoven separators is deposited at a high temperature (for instance, 180 °C), they could still keep the initial dimension steadily and could effectively avoid short circuit between the electrodes. So the nonwoven separators are now deemed as an important candidate for separators used in high power lithium ion batteries. However, the excessively large pore size and relatively weak interaction with liquid electrolyte usually cause internal short circuit, overgrowth of lithium dendrite, self-discharge and electrolyte leakage, which would further deteriorate the battery cycle performances and safety [5].

To resolve the limitations of the nonwoven separators, Zhu et al. [2] prepared a kind of poly(vinylidene fluoride) (PVDF) gel polymer electrolyte doped nonwoven separator. The gel part could effectively prevent liquid electrolyte leakage and provide a more intimate contact with the electrodes to enhance the interfacial stability [2]. However, the fully populated pores are not conducive to the rapid diffusion of the lithium ions, which might further restrict the improvement of battery power performances. Lee et al. [12–15] developed various kinds of colloidal particle and inorganic nanoparticle composite nonwoven separators. The introduction of the particles helped to decrease the pore size of the nonwoven substrate. Meanwhile, the well-connected interstitial voids between the particles could provide an easy access for liquid electrolyte penetration and lithium ion transportation. But they have also pointed out that long-term durability of this kind of composite nonwoven separators, especially for the colloidal particle embedded nonwoven separator, still needs more considerations. [13] To effectively avoid the shortcomings of large pores on the surface, at the same time to play the advantage of the high porosity of the nonwoven separator and to provide a more stable modification layer, a new kind of sandwich-like composite separator (Fig. 1) was designed in this work. Crosslinked polyethylene glycol (PEG) layer was introduced onto both sides of the nonwoven separator by in situ polymerization, which could firmly lock the surface nonwoven fabric and further improve the long-term durability of the composite separator. The surface pore size could also be effectively decreased, which could alleviate liquid electrolyte leakage and restrict the growth of lithium dendrite. [16] The remained large pores in the interior of the composite separator were expected to provide quick access for lithium ion and to make contribution for the superior rate capability of lithium ion batteries. The content of the crosslinked PEG was changed, and the morphology changes and electrochemical performances of the composite separators were explored.

2. Experimental

2.1. Materials

Polypropylene (PP) separator with 42% porosity (20 μm) was bought from Donghang Optoelectronics Technology Co., Ltd., China. PI nonwoven substrate was kindly provided by Jiangxi Xiancai Science and Technology Co., Ltd., China. The thickness is 38 μm, and the porosity is about 80%. Poly(ethylene glycol) methyl ether acrylate (PEGMEA, $Mn = 700$) and Poly(ethylene glycol diacry) (PEGDA, $Mn = 700$) were supplied by Aladdin Reagent Company. 2, 2′-Azobis (2-methylpropionitrile) (AIBN) and acetone were obtained from Sinopharm Chemical Reagent Co., Ltd, China. PEGMEA, PEGDA and AIBN were purified before use. The electrolyte solution of $LiPF_6$ (1 mol L^{-1}, SZ-SSDE-NIM-006, ion conductivity 10^{-2} S cm^{-1} at 25 °C) was provided by BASF Battery Materials (Suzhou) Co. Ltd., China.

2.2. Preparation of the sandwich-like composite separators

Proportional PEGMEA, PEGDA and AIBN were added in acetone and were then stirred to be homogenous at room temperature. The composition of the mixed coating solution was shown in Table 1. The monomer solution impregnated non-woven fabric was obtained by a traditional dip-coating method. The nonwoven substrate was immersed in the monomer solution for 2 min and was then draw out through a slit (45 μm) to remove redundant solution. The obtained film was heated at 60 °C in the oven for 6 h. In this process, a free-radical addition reaction between PEGMEA and PEGDA would happen, and the crosslinked PEG skin layer would be formed on both sides of the nonwoven substrate. Solvent evaporation would take place simultaneously. A series of sandwich-like composite separators were finally achieved. The corresponding codes are listed in Table 1.

2.3. Characterizations of the sandwich-like composite separators

The SEM photographs were obtained by field emission scanning electron microscopy (FESEM) (S-4800, Hitachi) after samples were coated by gold. Gurley value (sec 100 cc^{-1}) was achieved by
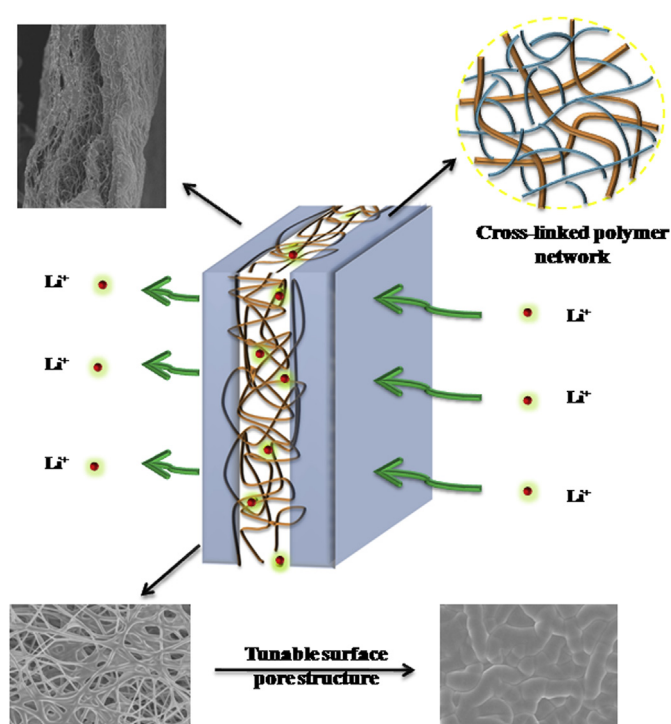

Fig. 1. Schematic principle of the sandwich-like composite separator for lithium ion batteries.

Table 1
Composition of the monomer solutions and the corresponding code of the composite separators.

Code	Solution composition				Monomer concentration (wt%)	Thickness (μm)
	PEGMEA (g)	PEGDA (g)	AIBN (g)	Acetone (g)		
A	0.00	0.00	0.00	0.00	0	38.0
B	0.80	0.20	0.018	9.00	10	39.9
C	1.60	0.40	0.020	8.00	20	40.6
D	1.80	0.45	0.022	5.25	30	42.2
e	2.40	0.60	0.024	4.50	40	42.8

determining the time for air to pass through a settled volume (30 ml) under a given pressure. [17] A home-made instrument with an airtight tank used for membrane sealed and a vent with a pressure gauge was used. The electrolyte uptake (U) was calculated by the equation $U(\%) = 100 \times (M-M0)/M0$, where $M0$ and M represents the weight of the dry and liquid electrolyte wetted gel separator, respectively. The retention ratio (R) was defined as the ratio of the electrolyte uptake at a fixed time and the initial uptake, which could be calculated according to the equation $R(\%) = 100 \times (Mi-M0)/(M-M0)$, where Mi represents the weight of the wetted separator after being kept for a fixed time. The determination was operated at the glove box, which is filled with Ar. Separators with saturated liquid electrolyte were placed in the glove box and the uptake amount was measured at a regular time. The bulk impedance (R_b) of the gel separator was determined by an electrochemical work station system (CHI660e, China) with the assembly of stainless steel (SS)/gel separator/SS. The ion conductivity (σ) was calculated by $\sigma = d/(R_b \times A)$, where d and A are the thickness and the effective area of the separator, respectively. The interfacial resistance (R_{int}) was determined with the assembly of lithium/composite separator/lithium on the electrochemical work station system (CHI660e, China). The cathode containing the

LiFePO$_4$, super P and PVDF with a mass ratio of 9:0.5:0.5 (wt/wt/wt) was prepared. The cycling performances were tested with the LiFePO$_4$ based cathode (content in each coin cell being about 7 mg) and lithium anode. Assembled coin cells were cycled on a cell testing system (LAND CT2001A, China) between 2.5 V and 4.2 V under different current rates.

3. Results and discussion

The surface and cross-section morphologies of the composite separators and the commercialized PP separator were characterized by SEM and are shown in Fig. 2. The original PI nonwoven separator (separator ID: a) has many open pores on the surface layer and the pore size is about 5 μm. As shown in Table 1, the content of the crosslinked PEG is controlled by the monomer concentration. When the crosslinked PEG was introduced and the monomer concentration was elavated, the surface pore size decreases obviously. When the monomer concentration reaches 40 wt %, the pores on the surface of separator e are totally covered. The inset gives the cross-section photographs of the separators. The crosslinked PEG formed skin layers on the separators and the thickness of the skin layer increases when the monomer
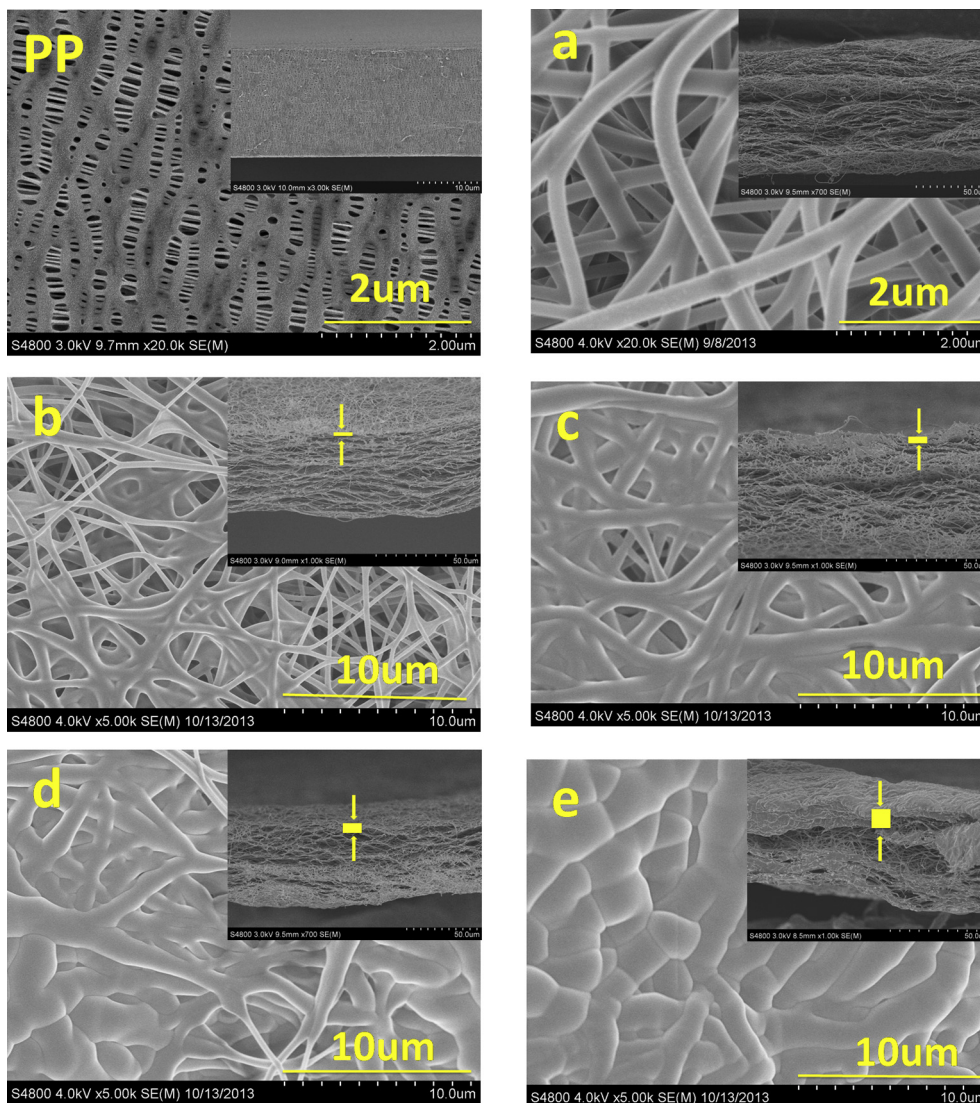

Fig. 2. Surface and cross-section (inset) FE-SEM images of the commercial PP separator, the nonwoven substrate (a) and the composite separators (b–e).

concentration is raised. The skin layer is formed through dip-coating firstly and then in-situ polymerization process. So the increase of the thickness of the skin layer corresponds to the decrease of the thickness of the porous interlayer in the composite separators. Influences of the separator structure change on the electrochemical performances would be explored detailedly in the following text. The commercialized PP separator, which is prepared by uniaxial stretching process, was used as a reference. The PP separator has a typical slit-like pore structure with pore size being about 0.2 μm.

The pore structure change was further quantificationally characterized by the Gurley value, which is defined as the time for air to pass through a settled volume under a given pressure. [17] Generally, a high Gurley value means relatively tortuous pore structure and low air permeability [18]. Fig. 3 gives the determination results. The PI nonwoven separator (separator ID: a) has large pore size and high porosity, so the determined Gurley value is beyond limitation when the test pressure is 0.02 MPa. Gurley value shows an increasing trend when the crosslinked PEG was introduced. For separator e, the Gurley value reaches 214 sec 100 cc^{-1}. This phenomenon could be easily explained by the SEM observation, that the pores on the surface layer are gradually covered. The Gurley value of the PP separator is 116 sec 100 cc^{-1}. It could be deduced that separator a and separator b have a shorter tortuous path for air transport than PP separator, which could be attributed to the highly porous structure of the nonwoven separators.

The introduced crosslinked PEG content was calculated by determining the weight increase and shown in Fig. 4(a). When the monomer concentration is raised, the crosslinked PEG content in the composite separator also increases, which suggests that the composition of the composite separators is controllable. The liquid electrolyte uptake of the composite separators and the PP separator was also determined. It could be seen that the electrolyte uptake decreases obviously when the crosslinked PEG content increases. The reason lies in that the crosslinked PEG could be swelled by the liquid electrolyte and then form the gel polymer electrolyte. [19] The swollen PEG gel would depress the space (pores) for liquid electrolyte. Due to the porosity of the nonwoven separator is fixed, introduce of the PEG gel into the nonwoven separator would
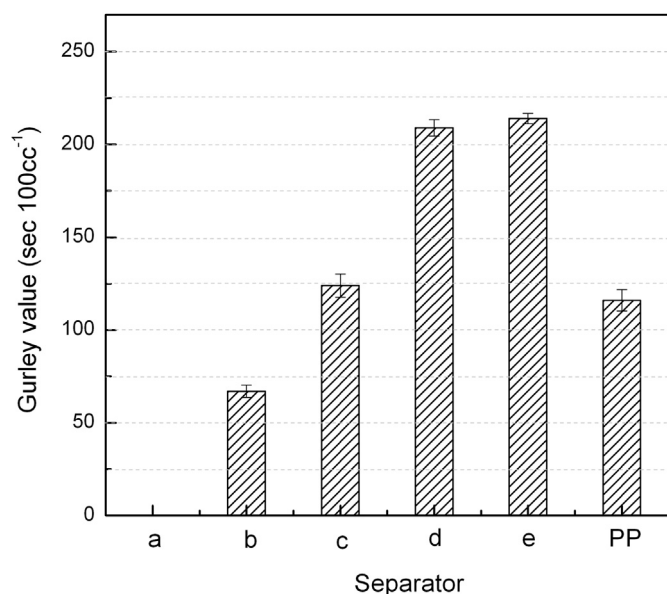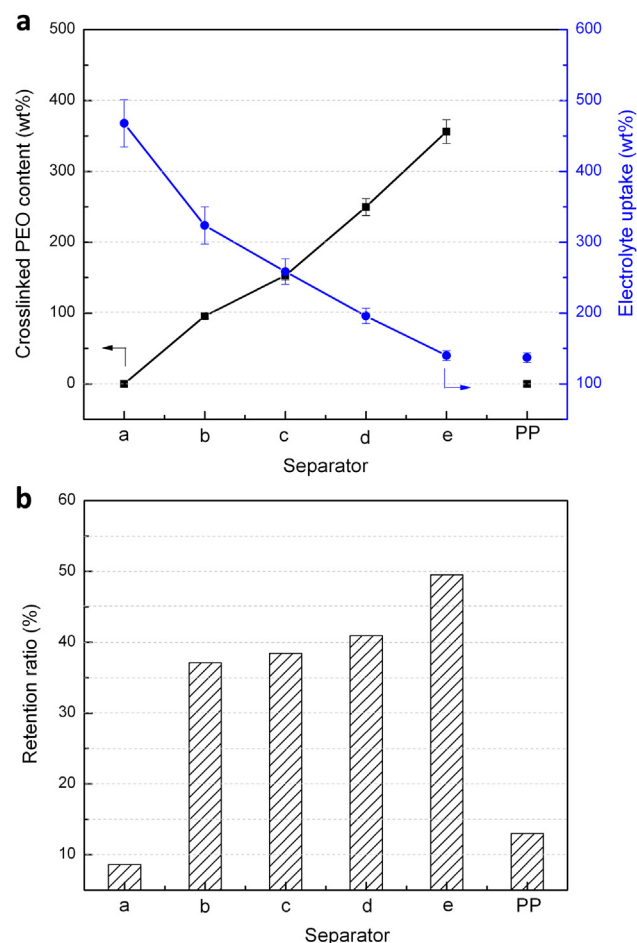

Fig. 4. (a) The crosslinked PEG content and liquid electrolyte uptake of the composite separators and PP separator; (b) the electrolyte retention ratio of the composite separators and PP separator after 15 h.

absolutely reduce the pore number for liquid electrolyte storage, yielding deceased whole uptake. [20] However, it should be noticed that all the composite separators show higher electrolyte uptake than the commercialized PP separator. The electrolyte uptake of separator e is 140%, while the uptake for PP separator is 137%. The discrepancy comes from the very high porosity (≈80%) of the PI nonwoven substrate, which is about two times from that of PP separator.

A big concern for the pristine nonwoven separator is the liquid electrolyte leakage due to the excessively large pore size and relatively weak interaction between the separator and the liquid electrolyte, which would threaten battery cyclability and safety greatly [15,21]. Introduction of the crosslinked PEG skin layer was expected to enhance the stability of the liquid electrolyte entrapped in the composite separators. The stability was characterized by the retention ratio, which is defined as the percentage of the uptake after the wetted separators being exposed in the glove box for 15 h with the initial saturated electrolyte uptake. As can be seen in Fig. 4(b), the retention ratio of the composite separators increases with increasing PEG content, suggesting the liquid electrolyte is more stable in the composite separator. The reason lies in decreased pore size on the surface layer of the composite separator and enhanced interaction between PEG and liquid electrolyte [15]. Meanwhile, compared with the commercialized PP separator, the composite separator still show excellent retention capacity for liquid electrolyte.
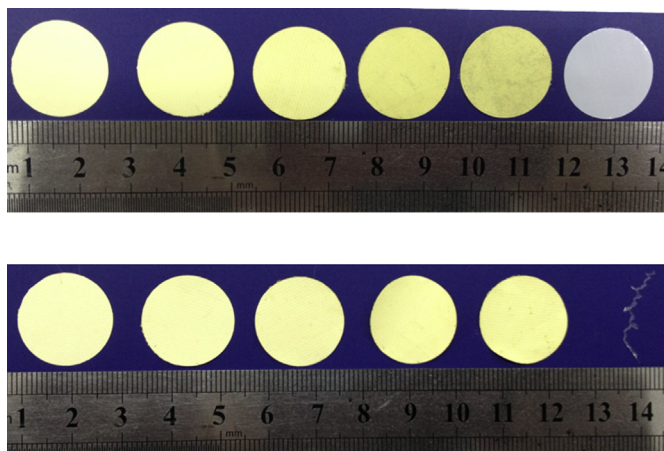

Fig. 3. The Gurley value of the composite separators and the commercialized PP separator (pressure: 0.02 MPa, area: 0.78 cm^2).

Fig. 5. Photograph of the thermal shrinkage of the composite separator and PP separator after being treated at 180 °C for 0.5 h.

Thermal stability and the flame retarding ability of the separators play an important role for battery safety [2,22]. The heat resistance of the composite separators was evaluated and compared with the commercial PP separator. All samples were deposited at 180 °C for 0.5 h at an oven and the dimensional change was recorded. As shown in Fig. 5, sizes of all the composite separators hardly change, while the PP separator has completely melted down. The superior thermal stability for the composite separators comes from the very high melting temperature (>250 °C) of the PI nonwoven matrix. So the composite separators are deemed to be a good solution to effectively avoid short circuit between the electrodes when the lithium ion battery is at a relatively high temperature (for instance, 180 °C).

Fig. 6 gives the results of the flame retarding test of the PP separator and the composite separator c. After being exposed to the fire, the PP separator shrank immediately and then caught on fire. Finally, the separator completely burned out. The composite separator c owned good flame retardant property. Due to the temperature of the fire were very high, the composite separator still showed obvious shrinkage. However, they were hard to catch on fire and showed the characteristics of self-extinguishing, which is attributed to the PI matrix. To get better understanding of the test, the videos are given in the supporting information. The thermal resistance test and the flame retarding test suggest that the composite separators could contribute higher safety to the lithium ion batteries than the traditional polyolefin separators.

Supplementary video related to this article can be found at http://dx.doi.org/10.1016/j.jpowsour.2014.07.151.

Video 1 corresponds to the "Video of the flame test of PP separator" in the accepted manuscript.

Video 2 corresponds to the "Video of the flame test of composite separator" in the accepted manuscript.

Fig. 7 gives the Nyquist plot and calculated ion conductivity of the separators. The impedance could be retrieved from the intercept of the Nyquist plots. [2] It is observed that the impedance increases when the content of crosslinked PEG is elevated (Fig. 6(a)). Correspondingly, the ion conductivity at ambient temperature shows a decrease trend (Fig. 7(b)). This is because lithium ion transportation is more difficult in gel polymer electrolyte than in the liquid electrolyte [17]. The increased content of crosslinked PEG (the skin layer) would yield higher amount of gel polymer electrolyte component in the composite separators when they are activated by the liquid
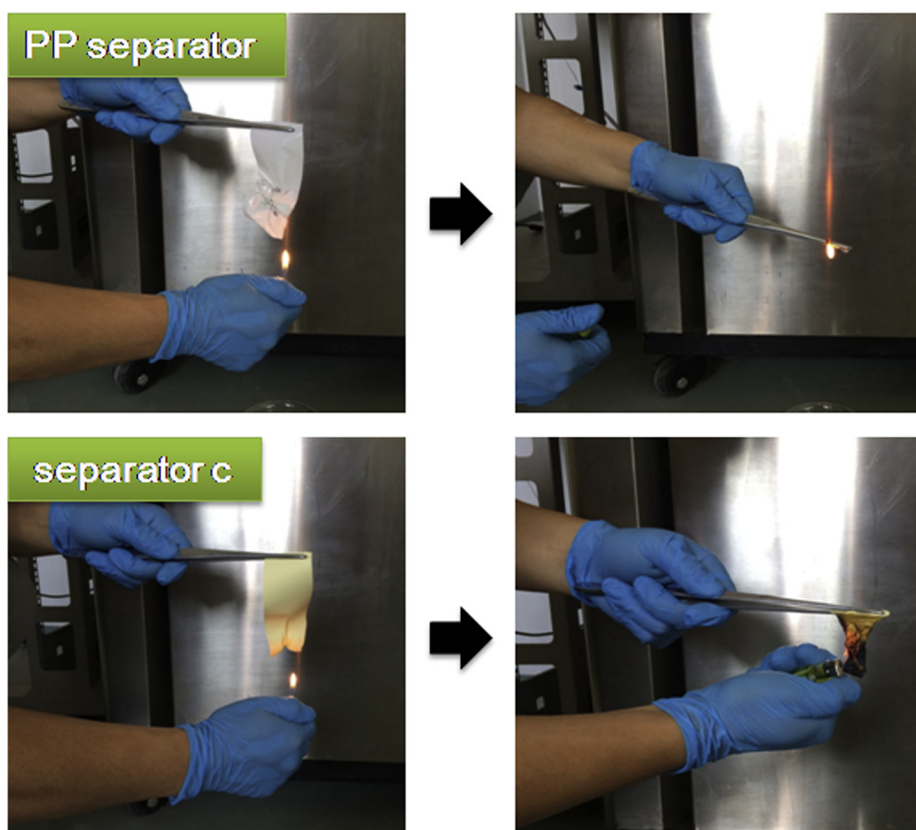

Fig. 6. The flame retarding test of the PP separator and the composite separator c.
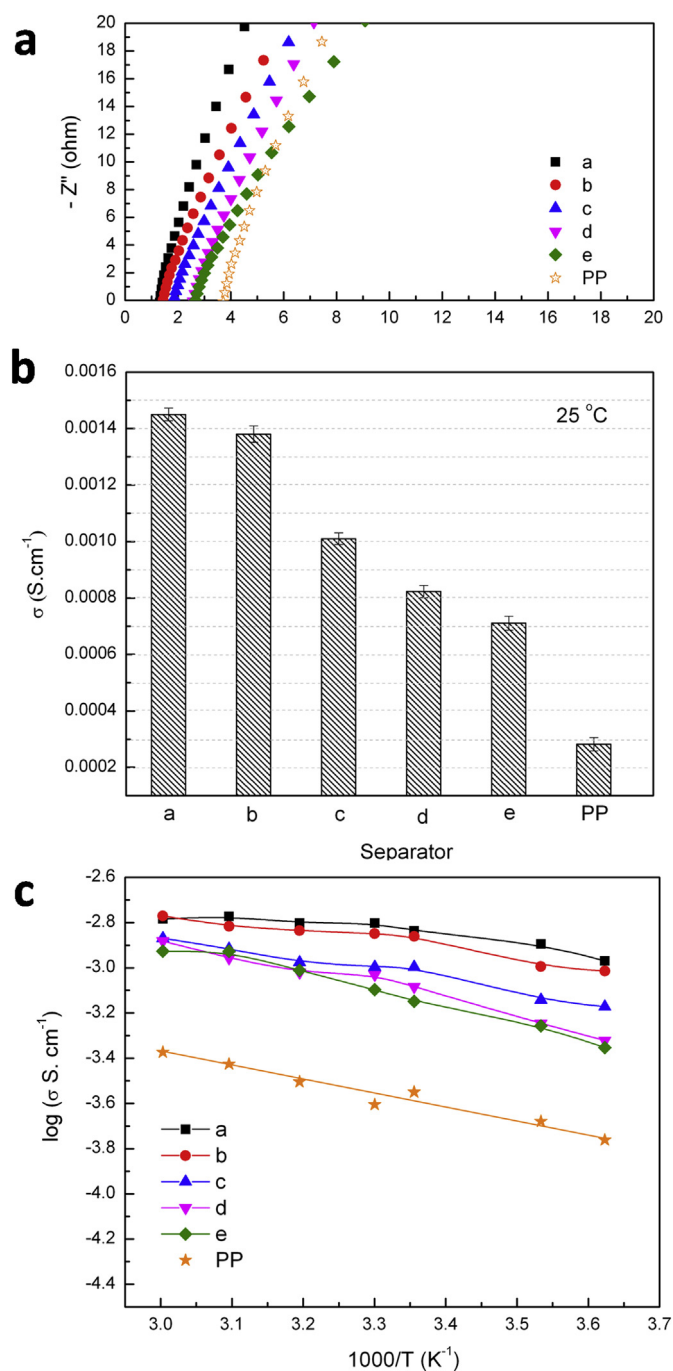
Fig. 7. (a) The Nyquist plots of the cells containing composite separators and PP separator; (b) the calculated ion conductivities at 25 °C; (c) The temperature dependence of the ion conductivities of the composite separators and PP separator.

temperature range is 3–60 °C. The logσ-1/T curve of PP separator is linear, suggesting that the temperature dependence of ionic conductivity can be described by Arrhenius model and the lithium ion migration for PP separator mainly occurs in the pores in the state of liquid electrolyte [23]. The logσ-1/T curves of the composite separators gradually become non-linearity (especially for separator e) when the crosslinked PEG content increases, indicating that the composite separators own the characteristic of the gel polymer electrolyte [19]. This is due to the existence of the gel skin layer. Even so, it's worth noting that the composite separators with the characteristics of gel polymer electrolyte still show higher ion conductivity than the commercialized PP separator.

Introduction of the gel skin layer is expected to improve the interfacial compatibility of the separator and the electrodes. [24] The interfacial compatibility was evaluated by the interfacial resistance (R_{int}) and its stability in the assembly of lithium/separator-electrolyte/lithium. As shown in Fig. 8, the Nyquist plots determined when the cells were assembled and stabled at normal temperature for 0, 3, 6, 10 days are obtained, which is fitted by the circuit diagram shown in Fig. 8(a) inset [16]. The large semicircle represents the interfacial resistance (R_{int}). For all the separators, R_{int} decreases first than increases. The reason lies in that the interfacial layer and the electrodes need time to be fully wetted by the electrolyte and to form a more convenient access for lithium ion transport in the interfacial layer.

Besides, the stabilized R_{int} (at 3rd day) of the composite separators increases with the raised PEG content in the skin layer. This result is quietly different with previous reports, in which the reported R_{int} usually decreased when the polar modification layer was introduced [17,25]. Generally, the reduce is considered to be the result of the enhanced intimate contact between the modification layer of the separator and the electrodes and the formation of a more uniformly wetted interface layer, which is beneficial for lithium ion transportation. However, in this work, the interfacial resistance is believed to be strongly dependent on the mobility of lithium ion at the surface layer of the separator. Since the gel layer was introduced on the nonwoven substrate surface, the migration ability of lithium ion at the modified separator surface layer weakens. So R_{int} increases. Due to the migration of lithium ion at the interfacial layer of PP separator and electrode being in the form of liquid electrolyte, a lower R_{int} is obtained. This result might give a new insight to the interfacial properties between the separator and electrodes.

Since good compatibility between separator and electrodes is also an essential factor to guarantee an acceptable performance in batteries [26], the interfacial compatibility was investigated and represented by the stability of interfacial resistance. The impedance change is obvious reduced when the gel skin layer was introduced. The change is 18 ohm for PP separator, 15 ohm for separator a and 12 ohm for separator e, which suggesting that the gel skin layer is conducive to the interfacial stability of separator and lithium electrode. The explanation is that the gel skin layer could give enhanced stability of liquid electrolyte in the interfacial layer and finally yields a permanent uniformly wetted interfacial layer, which could provide a convenient access for lithium ion transportation.

The electrochemical performances of the coin cells containing the composite separators and the commercialized PP separator were evaluated. The cells were charged/discharged at various current rates under the voltage range of 2.5–4.2 V. Due to the excessively large pore size of separator a causing internal short circuit, the electrochemical performances of cells containing separator a could not be obtained. Fig. 9(a) gives the C-rate capacities of the cells. When the discharge current rate is below 0.5C, no significant differences are observed for the discharge capacity of cells containing different separators. However, when the current rate is
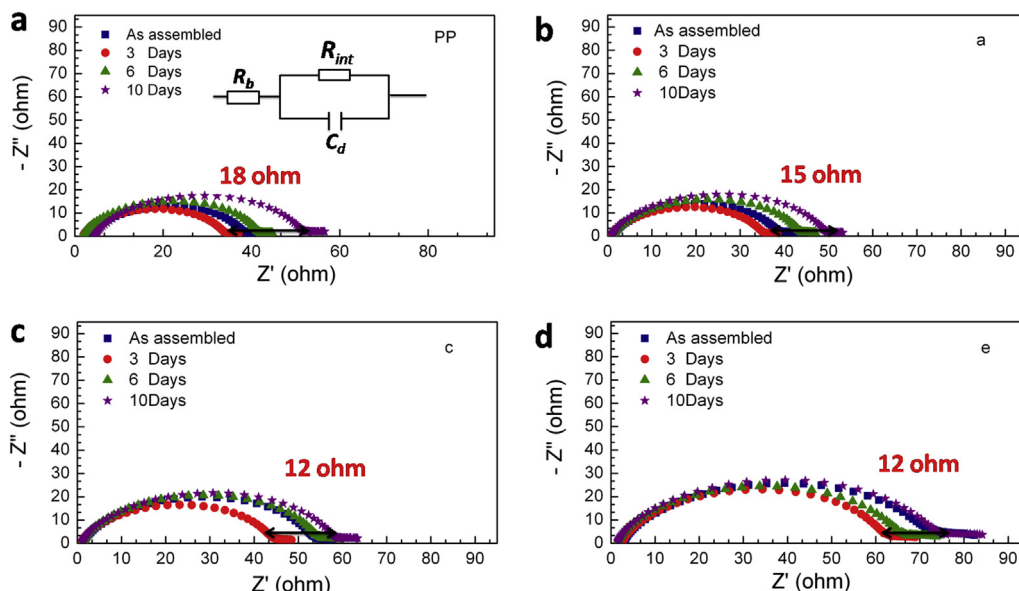
electrolyte. Meanwhile, the content of electrolyte in liquid state decreases. So the total ionic conductivity of the composite separators is reduced. However, the ionic conductivity of all composite separators is much higher than that of PP separator (0.28×10^{-3} S cm^{-1}). The ion conductivity of separator a is 1.45×10^{-3} S cm^{-1}, and the ion conductivity of separator e is 0.71×10^{-3} S cm^{-1}. Higher ion conductivity is attributed to the remained large pores in the interior of the composite separators, which is more conducive to C-rate capacity of the lithium ion batteries.

Fig. 7(c) shows the temperature dependence of the ion conductivity of the composite separators and PP separator. The

Fig. 8. Interfacial resistance and its stability of Li/separator soaked with liquid electrolyte/Li cells, a: PP separator, b: separator a, c: separator c, d: separator e.

higher than 0.5C, the discrepancy appears. The discharge capacity of cells containing separator e shows a dramatic drop. Generally, the C-rate capacity is deemed to be strongly dependent on the ion conductivity of the separator. [3,27] However, although the ion conductivity of separator e is much higher than that of the commercialized PP separator, the discharge capacity is far below that of PP separator. The reason is considered to be higher interfacial resistance for separator e (referring Fig. 8). Since the discharge capacity at higher current rate strongly relies on the mobility of lithium ion between the cathode and the anode [19], the influence factors of separator on the C-rate capacity should include the ion conductivity (mobility of lithium ion inside the separator) and the transport ability of lithium ion in the interfacial layer between the separator and the electrodes. The result in this work suggests that the interfacial resistance (compatibility) of separator and electrodes show a more significant associate with the C-rate performance than ion conductivity. Cao et al. [28] have expressed similar view on gel polymer electrolyte. The work further certifies that separator owns similar influence rule on the C-rate performance of the lithium ion battery.

Separator c shows the highest discharge capacity at the current rate of 2C and 3C. The explanation is that separator c owns higher ion conductivity and lower interfacial resistance than separator d and e, which is favorable for the fast and repeated lithium ion intercalation/de-intercalation in/from the electrodes, yielding higher battery capacity at high current rate [19]. Although the ion conductivity of separator b is higher than that of separator c, and according to the results of Fig. 8, the initial interfacial resistance of separator b should also be lower, the large pore size on separator surface might help the overgrowth of lithium dendrite during the cycling. So after several cycles at low current rates, much more lithium dendrite might be formed in the interfacial layer of separator b and electrodes, giving birth to a rapid increase of the interfacial resistance and lower discharge capacity at high current rates. As shown in Fig. 9(b) and (c), the initial discharge capacity of separator c is 158.7, 149.4, 144.4, 138.3, 127 and 117.2 mAh g^{-1} at 0.1, 0.3, 0.5, 1, 2, 3C rate, respectively, which is much higher than that of the commercialized PP separator (154.9, 157.1, 146.8, 134.6, 122.2, 100.8 mAh g^{-1} at 0.1, 0.3, 0.5, 1, 2, 3C rate, respectively). The results indicate that higher ohmic polarization is detected for cells

containing PP separator. The disparity comes from higher ion conductivity and a more stable interfacial layer for separator c in the cells. It should also be noticed that the discharge capacity at 3C of the coin cells containing the composite separators is higher than previous reports [13,18]. For example, Jeong et al. [15] have reported a kind of nano-particle embedded nonwoven composite separator. The discharge capacity at 2C is about 80 mAh g^{-1} (charged at 0.2C). The improved C-rate capacity is attributed to the sandwich-like separator structure with remained large pores in the interior of the composite separators.

The cyclability of the cells containing the composite separators and PP separator was characterized at a constant charge/discharge current density (1C/1C). As shown in Fig. 10, the initial discharge capacities of the cells containing separator b, c, d, e separators and PP separator are 133.6, 134.2, 133.6, 117.1 and 125.7 mAh g^{-1}, respectively. However, the coin cells containing PP separator show obvious attenuation during cycling. On the whole, the discharge capacity of the cells with separator b, c and d is higher than that of separator e and PP separator. The above variation of the discharge capacity of the composite separators is same with that of the C-rate capacity at high current rate, causes of the variation as above. The discharge capacity of PP separator shows a more obvious drop with increasing cycle number. The retention ratio is about 78.4% after 100 cycles. In comparison, cells containing the composite separators own higher discharge capacity retention ratio. Improved cell's capacity retention for the composite separators is attributed to enhanced interfacial stability and stronger affinity between the composite separator and liquid electrolyte (Fig. 4(b)) [12,29]. The former could yield a more convenient ion transport access in the interfacial layer of the cell. And the later gives better electrolyte retention during cycling, yielding a higher capacity retention rate.

After comprehensive comparison, the composite separator c prepared with 20 wt% coating solution is considered to be the most promising candidate for the high power high safety lithium ion battery.

4. Conclusions

A new kind of sandwich-like composite separators is developed in this work. For the composite separators, crosslinked PEG layer is
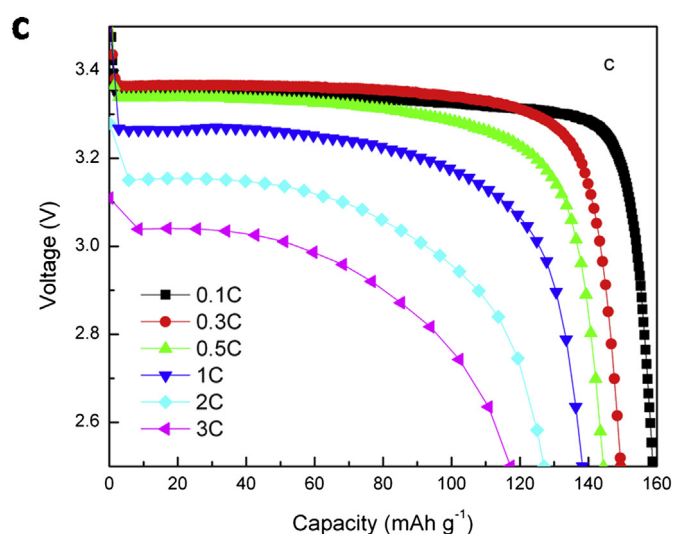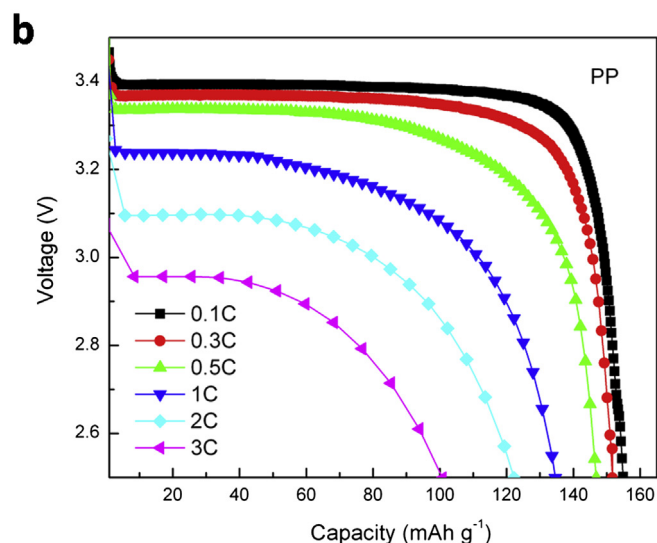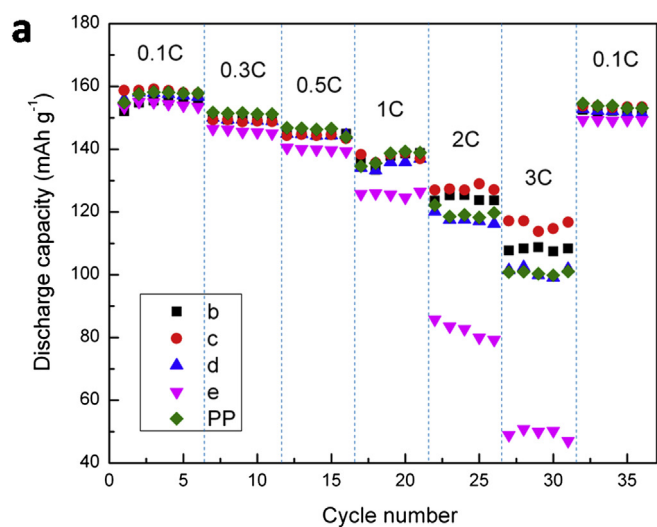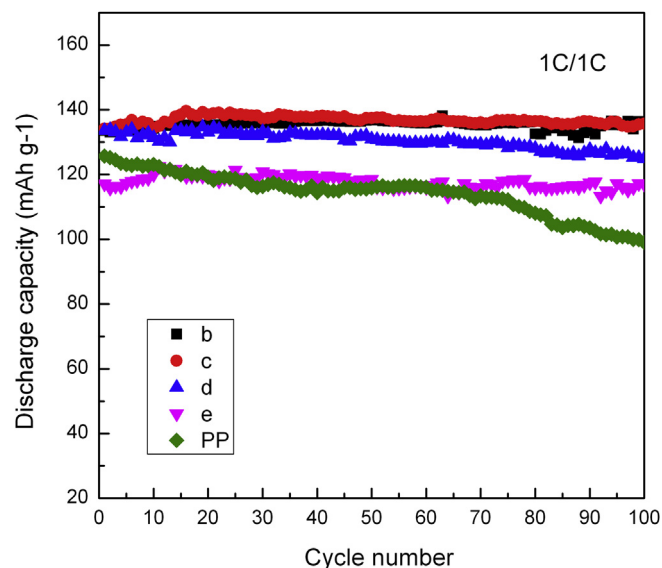
Fig. 10. The discharge capacity of cells containing the composite separators and PP separator.

introduced onto both sides of the nonwoven separator by in situ polymerization and the large pores in the interior of the composite separator are remained. The composite separators have several favorable properties, such as high ion conductivity, enhanced wettability with liquid electrolyte, high thermal stability, good flame retardant property and improved compatibility with the electrodes, yielding superior C-rate capability and cyclability, which makes them suitable for the usage in the high power/high energy lithium ion batteries with high safety level. The present work demonstrates that the tunable porous structure of the sandwich-like composite separators plays an important role in determining separator properties and cell performances. A notable contribution of this study is providing a new concept for the structure-design and fabrication of high performance separators for high power high safety lithium ion batteries.

Acknowledgments

References

[1] J. Hassoun, B. Scrosati, Adv. Mater. 22 (2010) 5198–5201.
[2] Y.S. Zhu, F.X. Wang, L.L. Liu, S.X. Xiao, Z. Chang, Y.P. Wu, Energy Environ. Sci. 6 (2013) 618–624.
[3] J. Lee, C.L. Lee, K. Park, I.D. Kim, J. Power Sources 248 (2014) 1211–1217.
[4] P. Arora, Z.M. Zhang, Chem. Rev. 104 (2004) 4419–4462.
[5] J.H. Cho, J.H. Park, J.H. Kim, S.Y. Lee, J. Mater. Chem. 21 (2011) 8192–8198.
[6] J.H. Park, J.H. Cho, W. Park, D. Ryoo, S.J. Yoon, J.H. Kim, Y.U. Jeong, S.Y. Lee, J. Power Sources 195 (2010) 8306–8310.
[7] M. Xiong, H.L. Tang, Y.D. Wang, M. Pan, Carbohydr. Polym. 101 (2014) 1140–1146.
[8] J.J. Zhang, Z.H. Liu, Q.S. Kong, C.J. Zhang, S.P. Pang, L.P. Yue, X.J. Wang, J.H. Yao, G.L. Cui, ACS Appl. Mater. Interfaces 5 (2013) 128–134.
[9] J.L. Hao, G.T. Lei, Z.H. Li, L.J. Wu, Q.Z. Xiao, L. Wang, J. Membr. Sci. 428 (2013) 11–16.
[10] Y.E. Miao, G.N. Zhu, H.Q. Hou, Y.Y. Xia, T.X. Liu, J. Power Sources 226 (2013) 82–86.

Fig. 9. (a) Comparison of the discharge C-rate capacity of the cell containing different separators, (b) the discharge capacity of the cell containing PP separator and (c) the discharge capacity of cells containing the composite separators (the charge current rate is 0.1C).

[11] Y.Z. Liang, L.W. Ji, B.K. Guo, Z. Lin, Y.F. Yao, Y. Li, M. Alcoutlabi, Y.Q. Qiu, X.W. Zhang, J. Power Sources 196 (2011) 436−441.
[12] J.R. Lee, J.H. Won, J.H. Kim, K.J. Kim, S.Y. Lee, J. Power Sources 216 (2012) 42−47.
[13] E.S. Choi, S.Y. Lee, J. Mater. Chem. 21 (2011) 14747−14754.
[14] H.S. Jeong, E.S. Choi, S.Y. Lee, J.H. Kim, J. Membr. Sci. 415−416 (2012) 513−519.
[15] H.S. Jeong, E.S. Choi, S.Y. Lee, Electrochim. Acta 86 (2012) 317−322.
[16] H.S. Jeong, E.S. Choi, J.H. Kim, S.Y. Lee, Electrochim. Acta 56 (2011) 5201−5204.
[17] J.L. Shi, L.F. Fang, H. Li, H. Zhang, B.K. Zhu, L.P. Zhu, J. Membr. Sci. 437 (2013) 160−168.
[18] H.S. Jeong, J.H. Kim, S.Y. Lee, J. Mater. Chem. 20 (2010) 9180−9186.
[19] J. Li, Y. Lin, H.H. Yao, C.F. Yuan, J. Liu, ChemSusChem, doi: 10.1002/cssc.201400113.
[20] H. Li, X.T. Ma, J.L. Shi, Z.K. Yao, B.K. Zhu, L.P. Zhu, Electrochim. Acta 56 (2011) 2641−2647.
[21] S.H. Wang, S.S. Hou, P.L. Kuo, H. Teng, ACS Appl. Mater. Interfaces 5 (2013) 8477−8485.
[22] Q. Xu, Q.S. Kong, Z.H. Liu, J.J. Zhang, X.J. Wang, R.Z. Liu, L.P. Yue, G.L. Cui, RSC Adv. 4 (2014) 7845−7850.
[23] Z.Y. Cui, Y.Y. Xu, L.P. Zhu, J.Y. Wang, Z.Y. Xi, B.K. Zhu, J. Membr. Sci. 325 (2008) 957−963.
[24] I.C. Kim, K.H. Lee, J. Membr. Sci. 230 (2004) 183−188.
[25] Q.W. Lu, J.H. Fang, J. Yang, R.R. Miao, J.L. Wang, Y. Nuli, J. Membr. Sci. 449 (2014) 176−183.
[26] Y.J. Kim, H.S. Kim, C.H. Doh, S.H. Kim, S.M. Lee, J. Power Sources 244 (2013) 196−206.
[27] H.S. Jeong, S.C. Hong, S.Y. Lee, J. Membr. Sci. 364 (2010) 177−182.
[28] J. Cao, L. Wang, M. Fang, Y.M. Shang, L.F. Deng, J.P. Yang, J.J. Li, H. Chen, X.M. He, Electrochim. Acta 114 (2013) 527−532.
[29] Q. Xu, Q.S. Kong, Z.H. Liu, X.J. Wang, R.Z. Liu, J.J. Zhang, L.P. Yue, Y.L. Duan, G.L. Cui, ACS Sustain. Chem. Eng. 2 (2014) 194−199.